

Scientific paper

Preparation of $\text{Co}_x\text{Fe}_{3-x}\text{O}_4$ Oxydic System Starting from Metal Nitrates and Propanediol

Mircea Stefanescu,¹ Marcela Stoia,¹ Thomas Dippong,¹
Oana Stefanescu¹ and Paul Barvinschi²

¹ Faculty of Industrial Chemistry and Environmental Engineering, University "Politehnica" of Timisoara, P-ta Victoriei nr. 2., 300006, Timisoara, Romania

² Faculty of Physics, West University of Timisoara, Bv. V. Parvan no. 4, 300223 Timisoara, Romania

* Corresponding author: E-mail: mircea.stefanescu@chim.upt.ro

Received: 08-10-2008

Abstract

This paper presents a study on preparation of the oxydic system $\text{Co}_x\text{Fe}_{3-x}\text{O}_4$ ($x = 0,5; 1,0; 1,5$) as nanoparticles starting from metallic nitrates ($\text{Co}(\text{NO}_3)_2 \cdot 6\text{H}_2\text{O}$, $\text{Fe}(\text{NO}_3)_3 \cdot 9\text{H}_2\text{O}$) and diols: 1,2 propanediol ($\text{OHCH}_2\text{CH}(\text{OH})\text{CH}_3$) and 1,3 propanediol ($\text{OH}(\text{CH}_2)_3\text{OH}$). During the heating of metal nitrates – diol solution, a redox reaction took place between NO_3^- anion and polyol, when $-\text{CH}_2-\text{OH}$ was oxidized at $-\text{COO}^-$. The carboxylate anions, which resulted in the redox reaction, reacted with $\text{Co}(\text{II})$ and $\text{Fe}(\text{III})$ cations to form coordinative compounds, that were used as precursors for the $\text{Co}_x\text{Fe}_{3-x}\text{O}_4$ oxide system.

DTA curves of the solutions $\text{Co}(\text{NO}_3)_2 \cdot 6\text{H}_2\text{O}$, $\text{Fe}(\text{NO}_3)_3 \cdot 9\text{H}_2\text{O}$ – diol, showed two exothermic heat effects: at ~ 343 K, corresponding to the redox reaction $\text{Fe}(\text{NO}_3)_3$ – diol and at ~ 388 K, due to the redox reaction $\text{Co}(\text{NO}_3)_2$ – diol. As a result of these redox reactions, a homogenous mixture of $\text{Fe}(\text{III})$ and $\text{Co}(\text{II})$ carboxylate compounds was obtained. These oxides precursors have been characterized by thermal analysis and FT-IR spectrometry.

By thermal decomposition of the synthesized precursors at ~ 573 K, followed by annealing at 673 K, 973 K and 1273 K, CoFe_2O_4 was obtained as single or predominant nanocrystalline phase depending on the x value, as evidenced by XRD analysis.

Keywords: Cobalt ferrite, carboxylates, propanediol, thermal decomposition

1. Introduction

Spinel oxides described by the general formula AB_2O_4 , with A and B representing tetrahedral and octahedral sites exhibit interesting physical and chemical properties, depending on how the cations distribute among the A and B sites, sometimes in more than one ionic valence.¹

Spinel iron-cobalt oxide compounds may find useful applications in the change of thermoelectric power of cobalt ferrite in the hydrogen-deuterium exchange reaction or as catalysts for the hydrogen peroxide decomposition.² Cobalt ferrite nanoparticles CoFe_2O_4 are interesting because of their magneto-crystalline anisotropy, high coercivity, moderate saturation magnetization, high chemical stability, wear resistance and electric insulation.³ These

properties indicate a high physical and chemical stability. CoFe_2O_4 presents applications in microproduction industry, high performance digital tapes, refrigerators, ferrofluids, intensifying of magnetic resonance, etc.⁴

Cobalt ferrite crystallizes in a partially inverse spinel structure with the formula $(\text{Co}_\delta\text{Fe}_{1-\delta})[\text{Co}_{1-\delta}\text{Fe}_{1+\delta}]\text{O}_4$, and δ depends on thermal history. Since the $\text{Fe}_A^{3+} - \text{Fe}_B^{3+}$ superexchange interaction differs from the $\text{Co}_A^{2+} - \text{Fe}_B^{3+}$ interaction, variation of the cation distribution over the A and B sites in the spinel leads to different magnetic properties of the ferrite even for the same composition.⁵ The methods reported in the literature for preparation of cobalt ferrite nanoparticles with variable composition ($\text{Co}_x\text{Fe}_{3-x}\text{O}_4$) are: method of micro emulsions,⁶ co-precipitation,⁷ hydrothermal method,⁷ thermal decomposition of some precursors,⁸ combustion reaction method,³ etc.

Few studies have been reported in the literature on the system $(\text{Co}_x\text{Fe}_{3-x}\text{O}_4)$ as nanoparticles for large x (0.05–1.5) value ranges. These studies have followed the magnetic properties of the system in order to understand the high anisotropy of Co atoms in the spinel structure.⁹

In this paper we have studied the preparation of the oxidic system $\text{Co}_x\text{Fe}_{3-x}\text{O}_4$ for $x = 0,5; 1,0; 1,5$ starting from a mixture of Fe(III), Co(II) nitrates and diol: 1,2 propanediol (1,2 PG) and 1,3 propanediol (1,3 PG). During the heating of this mixture a redox reaction takes place between the nitrate ion and diol, when Co(II) and Fe(III) carboxylates form, which are further used as precursors of $\text{Co}_x\text{Fe}_{3-x}\text{O}_4$ oxides. We have studied the evolution of the crystalline phases with the annealing temperature, depending on the Co/Fe ratio introduced in synthesis and on the diols nature.

2. Experimental

The synthesis of Co(II) and Fe(III) carboxylate type complexes, precursors of cobalt ferrite, was achieved by a previously described method, based on the redox reaction between the nitrate ion and diols.^{10,11} The progress of the redox reaction was studied by thermogravimetric and differential thermal analysis on a MOM Budapesta derivatograph, up to 773 K. The solution was disposed in thin layer on Pt crucibles, for a sample mass of 100 mg, in static air atmosphere, with a heating rate of 5 K/min and $\alpha\text{-Al}_2\text{O}_3$ as reference material.

The precursors of cobalt ferrite were synthesized at 403 K using 1,2 PG and 1,3 PG for different molar ratios $\text{Fe}(\text{NO}_3)_3 : \text{Co}(\text{NO}_3)_2$, corresponding to the preparation of the $\text{Co}_x\text{Fe}_{3-x}\text{O}_4$ system for ($x = 0,5; 1,0; 1,5$) according to table 1.

All synthesized precursors were analysed by FT-IR spectrometry using a FT-IR Prestige-21, Shimadzu spectrometer, in the range 400–4000 cm^{-1} analysis with a MOM Budapesta derivatograph up to 800 K, using Pt crucibles.

We have decomposed the precursors ($\text{P}_1\text{--}\text{P}_6$) at 573 K, 3 hours and annealed at 673 K, 973 K and 1273 K, for 3 hours in a Nabertherm furnace, in static air atmosphere. The annealing products were characterized by XRD with

a diffractometer D8 Advanced-Bruker AXS, using Mo-K α ($\lambda_{\text{Mo}} = 0.7093 \text{ \AA}$) radiation and by FT-IR.

3. Results and Discussion

Our previous studies on the redox reaction $\text{Fe}(\text{NO}_3)_3$ – diol and $\text{Co}(\text{NO}_3)_2$ – diol,^{10,11} have evidenced that this reaction takes place at $\sim 343 \text{ K}$ for $\text{Fe}(\text{NO}_3)_3$ – diol and at $\sim 393 \text{ K}$ for $\text{Co}(\text{NO}_3)_2$ – diol with formation of Fe(III) and Co(II) carboxylates type complexes.

In this paper, in order to obtain precursors of the system $\text{Co}_x\text{Fe}_{3-x}\text{O}_4$, we have started from the mixture of the two metal nitrates ($\text{Fe}(\text{NO}_3)_3 \cdot 9\text{H}_2\text{O}$ and $\text{Co}(\text{NO}_3)_2 \cdot 6\text{H}_2\text{O}$) in different molar ratios and different diols (1,2PG and 1,3PG), according to table 1. The thermal behaviour of the metal nitrates ($\text{Fe}(\text{NO}_3)_3$, $\text{Co}(\text{NO}_3)_2$) and diol (1,2PG and 1,3PG) solutions was studied by DTA and TG.

Figure 1 presents the thermal curves for the mixture corresponding to the sample (P5) with 1,3 PG, at molar ratio $\text{Fe}(\text{NO}_3)_3 : \text{Co}(\text{NO}_3)_2 = 2 : 1$.

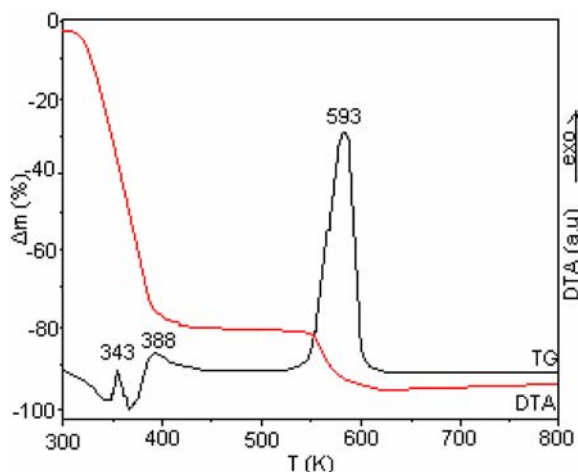


Figure 1. TG and DTA curves of the solution $\text{Co}(\text{NO}_3)_2\text{--}\text{Fe}(\text{NO}_3)_3\text{--}1,3\text{PG}$

Three exothermic effects were registered on DTA curve. The exothermic effect from 343 K (which overlaps with the endothermic effect due to the elimination of cry-

Table 1. Characteristics of the synthesized samples

Sample	Diol	Molar ratio $\text{Fe}(\text{NO}_3)_3 : \text{Co}(\text{NO}_3)_2$	Molar ratio $\text{NO}_3^- : \text{Diol}$	Calculated x value corresponding to $\text{Co}_x\text{Fe}_{3-x}\text{O}_4$
P1	1,2 PG	5:1	1:1	0,5
P2	1,2 PG	2:1	1:1	1,0
vP3	1,2 PG	1:1	1:1	1,5
P4	1,3 PG	5:1	1:1	0,5
P5	1,3 PG	2:1	1:1	1,0
P6	1,3 PG	1:1	1:1	1,5

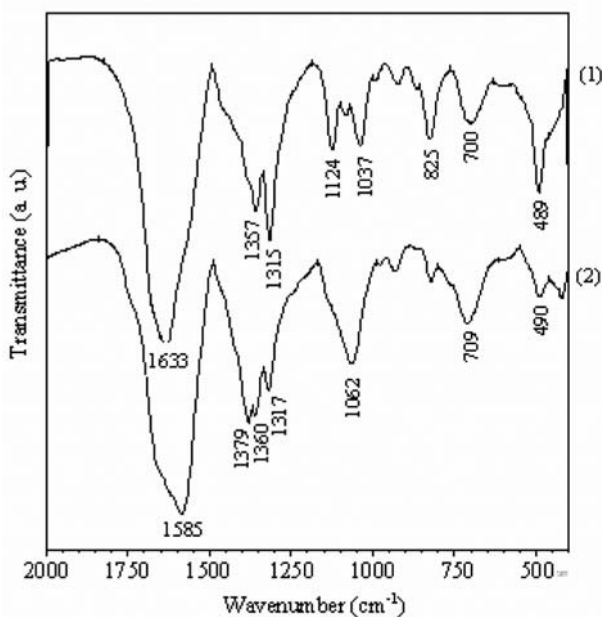


Figure 2. FT-IR spectra of the precursors P2 (1) and P5 (2) synthesized at 403 K

stal water) was attributed to the redox reaction $\text{Fe}(\text{NO}_3)_3 - 1,3\text{PG}$ and the effect from 388 K corresponds to the redox reaction $\text{Co}(\text{NO}_3)_2 - 1,3\text{PG}$.

The two stage evolution of the redox reaction in the mixture metal nitrates-diols is explained by the fact that the acvacation $[\text{Fe}(\text{H}_2\text{O})_6]^{3+}$ is a stronger acid than the acvacation $[\text{Co}(\text{H}_2\text{O})_6]^{2+}$. As a result, the redox reaction with formation of the corresponding iron carboxylates took place at lower temperatures. The result of these redox reactions was most probable the formation of a mixture of homonuclear Fe(III) and Co(II) carboxylates. The mass loss on TG, in this range, is due to the elimination of volatile products resulted in the redox reaction (H_2O , NO_2) and of the crystal water of the metal nitrates. The exothermic effect from 573 K is attributed to the oxidative decomposition of the carboxylates mixture with elimination of CO , CO_2 , corresponding to the mass loss in the range 523–573 K

All other synthesized samples exhibit similar TG and DTA curves with exothermic effects which depend on the ratio $\text{Fe}(\text{NO}_3)_3/\text{Co}(\text{NO}_3)_2$. Based on thermal analysis we have established 403 K as optimal synthesis temperature for the oxides precursors.

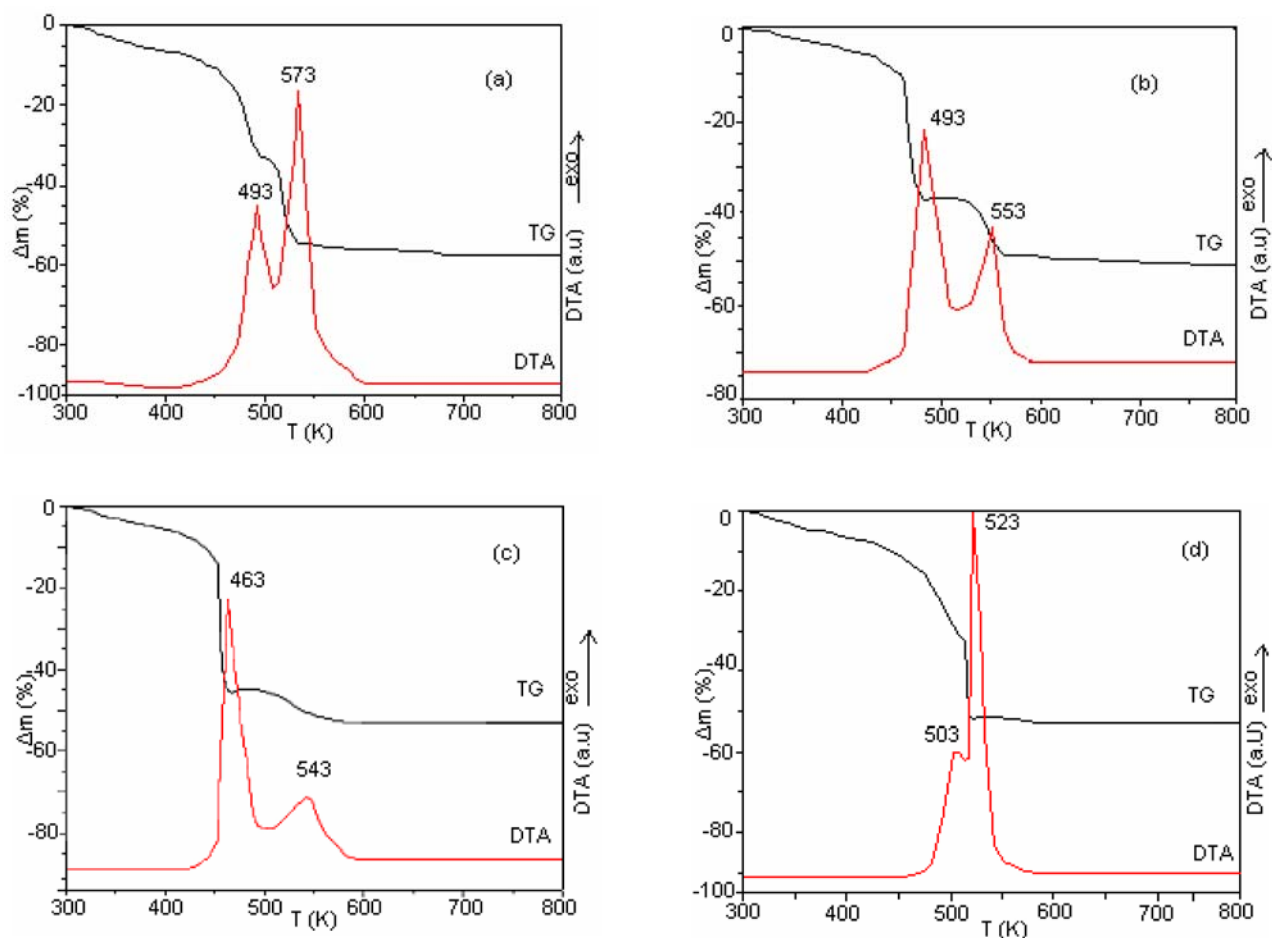


Figure 3. TG and DTA of the precursors synthesized at 403 K: (a) P1 (1,2PG, $x = 0.5$); (b) P2 (1,2PG, $x = 1$); (c) P4 (1,3PG, $x = 0.5$); (d) P5 (1,3PG, $x = 1$)

The obtained precursors were characterized using FT-IR analysis and thermal analysis. FT-IR analysis has evidenced the formation of metal carboxylates in all synthesized precursors. In figure 2 are presented the FT-IR spectra for the samples P2 (with 1,2 PG) and P5 (with 1,3 PG) for a molar ratio Fe(III) : Co(II) = 2 : 1 (corresponding to cobalt ferrite CoFe_2O_4).

The presence of the carboxylate group coordinated by the metal ions was evidenced by the characteristic bands: at $\sim 1600\text{ cm}^{-1}$ the band attributed to the vibration $\nu_{\text{as}}(\text{COO}^-)$ and in the range $1300\text{ cm}^{-1} - 1400\text{ cm}^{-1}$ the bands attributed to the vibrations $\nu_{\text{s}}\text{COO}^-$ ($\sim 1360\text{ cm}^{-1}$) and $\nu_{\text{s}}(\text{CO}) + \delta(\text{OCO})$ ($\sim 1320\text{ cm}^{-1}$).^{12,20} In case of the precursors synthesized with 1,2PG, a supplementary band appears at $\sim 1120\text{ cm}^{-1}$, characteristic for the secondary $-\text{OH}$ group, which did not interact with the nitrate ion during the redox reaction.¹³

The thermal behaviour of the synthesized precursors was studied by thermal analysis (TG and DTA). Figure 3 (a, b, c, d) presents the DTA and TG curves recorded at air heating up to 773 K, of the precursors synthesized with 1,2 PG (P1, P2) (figure 3(a) and 3(b)) and with 1,3PG (P4, P5) (figure 3(c) and 3(d)).

TG and DTA curves show that the oxidative decomposition of the precursors takes place in the range 573–673 K, in two stages. The exothermic effects on DTA in this temperature range correspond to the decomposition of the Fe(III) carboxylates (first effect) and Co(II) car-

boxylates (second effect) with formation of the oxides mixture. In the range 573–773 K the samples mass remains constant.

Our previous studies on the thermal decomposition of Fe(III) and Co(II) homonuclear carboxylates obtained with diols, have evidenced the in situ generation of a reducing atmosphere (CO) during the decomposition.^{10,11} This atmosphere determines the partial reduction of Fe(III) to Fe(II) and of Co(II) to Co(0) with re-oxidation to $\gamma\text{-Fe}_2\text{O}_3$,¹⁰ and to Co_3O_4 or CoO ,¹¹ in amorphous, very reactive state. These redox processes influence the obtaining of the $\text{Co}_x\text{Fe}_{3-x}\text{O}_4$ system.

Based on the thermal analysis data, the synthesized precursors were thermally decomposed at 573 K, 3 hours. In order to determine the evolution of the oxidic system $\text{Co}_x\text{Fe}_{3-x}\text{O}_4$ ($x = 0,5; 1,0; 1,5$) with the annealing temperature, the decomposition products were annealed at 573 K, 673 K, 973 K and 1273 K, for 3 hours. All samples were characterized by XRD and FT-IR.

In figure 4 are presented the XRD patterns for the sample P2 (with 1,2PG; $x = 1$) thermally treated at 573 K, 673 K, 973 K and 1273 K.

The XRD pattern for the decomposition product of the precursor P2 at 573 K (Figure.4 (1)) presented diffraction peaks characteristic to the spinel phases. The large and assymmetric bands suggest the existence of other spinel phases ($\gamma\text{-Fe}_2\text{O}_3$ and Co_3O_4) besides cobalt ferrite. By further annealing at 673 K, no significant changes can be

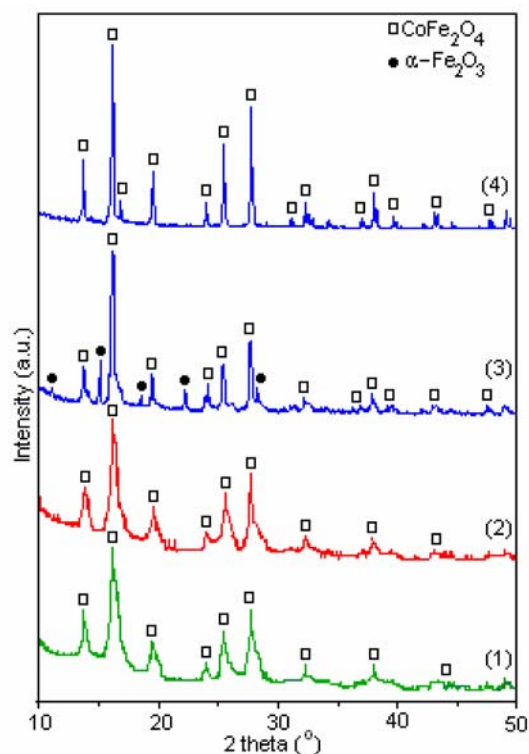


Figure 4. XRD patterns for the annealing products of the precursor P2 at 573 K (1), 673 K (2), 973 K (3), 1273 K (4)

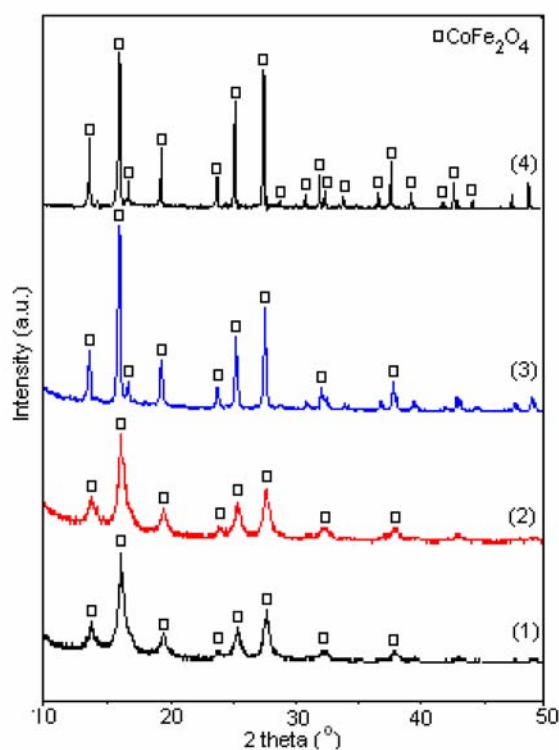


Figure 5. XRD patterns for the annealing products of the precursor P5 at 573 K (1), 673 K (2), 973 K (3), 1273 K (4)

observed regarding the nature and the crystallization degree of the oxides phases (Figure. 4, (2)).

The XRD pattern of the sample annealed at 973 K (figure.4, (3)) evidences besides the main crystalline phase CoFe_2O_4 , the hexagonal $\alpha\text{-Fe}_2\text{O}_3$ secondary phase. The later crystallises above 773 K from the spinel phase $\gamma\text{-Fe}_2\text{O}_3$,¹¹ which forms at low temperatures (573, 673 K). Pattern (4) of the sample annealed at 1273 K evidences the quantitative formation of CoFe_2O_4 as sole phase. At this temperature Co_3O_4 turns to CoO which reacts with $\alpha\text{-Fe}_2\text{O}_3$ to give cobalt ferrite. This confirmed the existence of Co_3O_4 in the powders obtained at lower temperatures.

Figure 5 presents the diffraction patterns of the powders obtained by annealing at 573 K, 673 K, 973 K and 1273 K of the precursor P5 (with 1,3PG, $x = 1$). The presented spectra evidence a single crystalline phase: CoFe_2O_4 spinel. The formation of cobalt ferrite as single phase starting with 573 K is due to the strong reducing atmosphere (CO) generated during decomposition, when amorphous, very reactive CoO and $\gamma\text{-Fe}_2\text{O}_3$ form.^{10,11} These phases interact at 573 K with quantitative formation of cobalt ferrite. The crystallization degree of cobalt ferrite increases with the annealing temperature.

From XRD data corresponding to the patterns presented in figures 4 and 5 we have estimated using the Scherrer equation, the mean diameters of the cobalt ferrite crystallites obtained at different temperatures from precursors P2 and P5. The obtained values are presented in table 2.

Table 2. Mean diameter values of the cobalt ferrite crystallites

Temperature (K)	Mean diameter (nm)	
	P2	P5
573	–	8
673	–	8
973	13	15
1273	18	20

The samples studied by XRD were also analyzed by FT-IR. The FT-IR spectra of the samples obtained by annealing the precursor P2 ($x = 1$) at different temperatures are presented in figure 6. Spectra (1) and (2) of the products annealed at 573 K and 673 K showed a strong band around $500\text{--}600\text{ cm}^{-1}$ characteristic to metal-oxygen bonds. This band with minimum at 580 cm^{-1} and shoulder at $\sim 670\text{ cm}^{-1}$ confirms the existence of $\gamma\text{-Fe}_2\text{O}_3$ and Co_3O_4 besides CoFe_2O_4 .^{14,15} Spectrum (3) of the sample annealed at 973 K exhibits a supplementary band at $\sim 460\text{ cm}^{-1}$, characteristic to the vibrations $\nu(\text{Fe} - \text{O})$ in $\alpha\text{-Fe}_2\text{O}_3$,¹⁶ along with the intense band from $\sim 580\text{ cm}^{-1}$. Spectrum (4) of the sample P2 annealed at 1273 K exhibits a symmetric strong band at 560 cm^{-1} , characteristic to cobalt ferrite CoFe_2O_4 ,¹⁷ sole phase at this temperature.

FT-IR spectra of the samples obtained by annealing the precursor P5 ($x = 1$) are presented in figure 7. All spectra have evidenced the presence of CoFe_2O_4 by the intense symmetric band from 585 cm^{-1} . In conclusion, the FT-IR

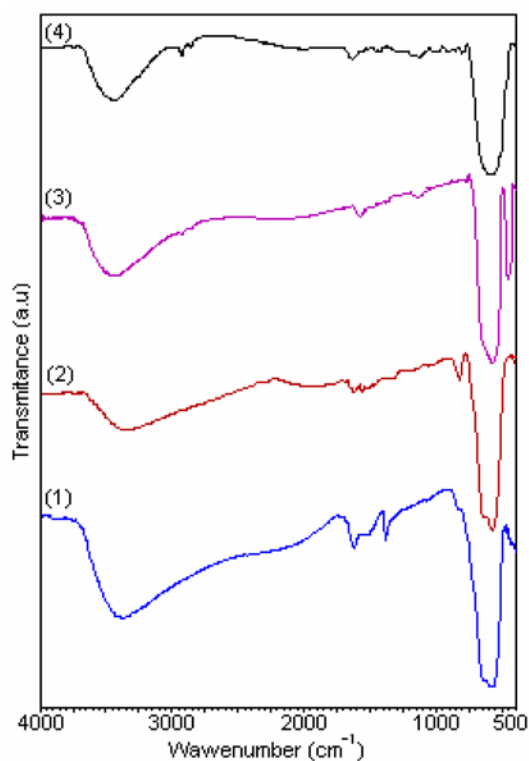


Figure 6. FT-IR spectra of the annealing products of the precursor P2 at 573 K (1), 673 K (2), 973 K (3), 1273 K (4)

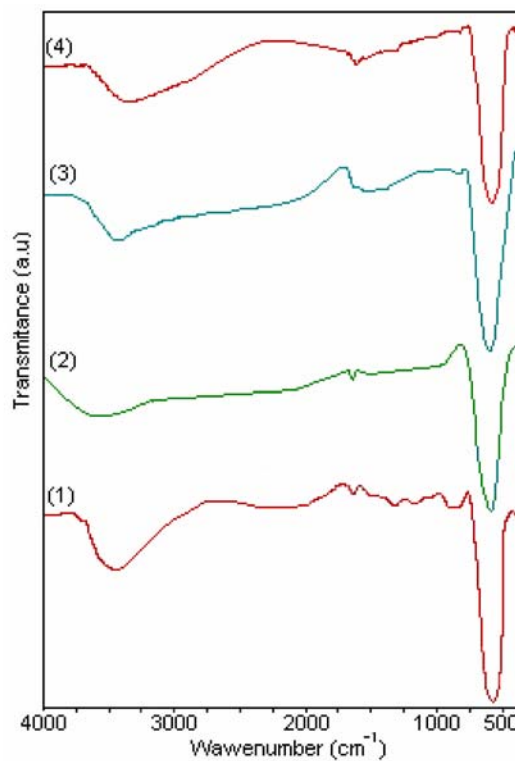


Figure 7. FT-IR spectra of the annealing products of the precursor P5 at 573 K (1), 673 K (2), 973 K (3), 1273 K (4)

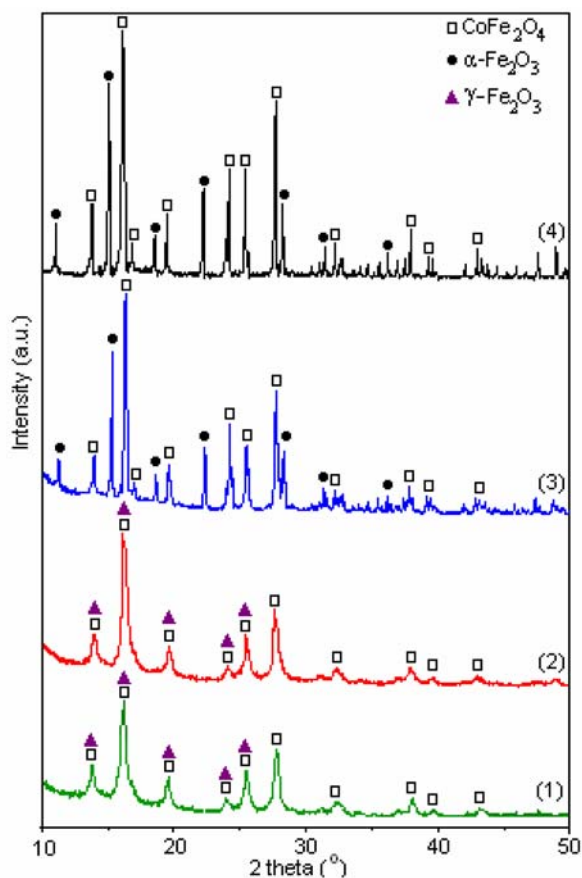


Figure 8. XRD patterns for the samples P1 annealed at different temperatures: 573 K (1); 673 K (2); 973 K (3); 1273 K (4)

study on the ferritic precursors of the annealing products from different temperatures confirmed the XRD study.

For $x \neq 1$, XRD analysis has evidenced the existence of other secondary phases besides cobalt ferrite. Figure 8 presents the XRD patterns of the samples obtained by annealing the precursor P1 (with 1,2PG, $x = 0.5$). The presented XRD patterns showed that the samples annealed at 573 K and 673 K (spectra 1 and 2) contains spinel phases (superposed lines of CoFe_2O_4 and $\gamma\text{-Fe}_2\text{O}_3$ corresponding to the iron excess). Patterns (3) and (4) corresponding to the samples annealed at 973 K and 1273 K have evidenced the presence besides the spinel CoFe_2O_4 of the secondary phase $\alpha\text{-Fe}_2\text{O}_3$ (formed by transformation of $\gamma\text{-Fe}_2\text{O}_3$). The same crystalline phases were evidenced in case of the samples obtained by annealing of precursor P4 (with 1,3PG, $x = 0.5$).

XRD patterns of the samples P3 (with 1,2PG) and P4 (with 1,3PG) with $x = 1.5$ are presented in figures 9 and 10. Spectra (1), (2) and (3) of the samples P3 annealed at 573 K, 673 K and 973 K and 1273 K presented in figure 9, evidence the lines of spinel phases: CoFe_2O_4 and Co_3O_4 (corresponding to the cobalt excess).

Pattern (4) of the sample annealed at 1273 K evidenced the diffraction peak characteristic to CoFe_2O_4 and al-

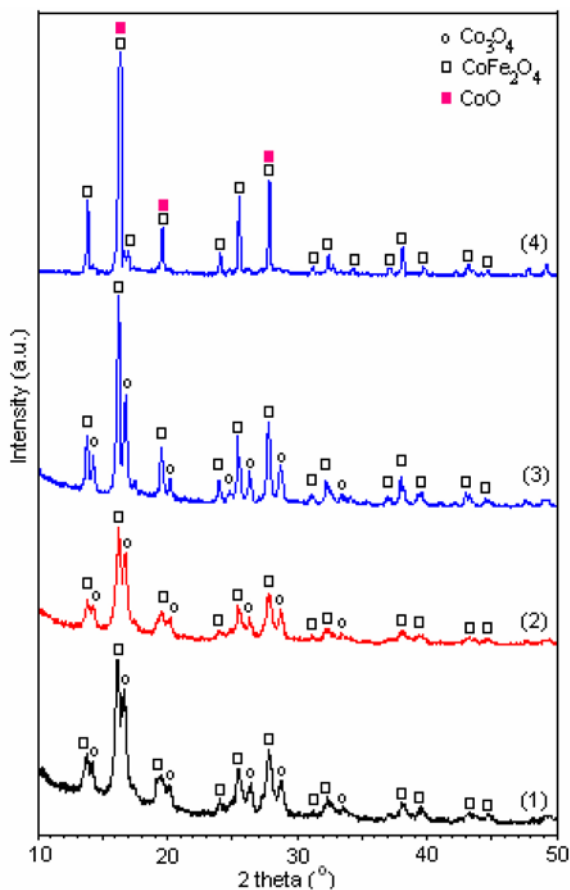


Figure 9. XRD patterns for the samples P3 annealed at different temperatures: 573 K (1); 673 K (2); 973 K (3); 1273 K (4)

so to CoO , which results from the transformation at ~ 1173 K of Co_3O_4 . The RX diffraction peaks of CoO are very close to the ones of CoFe_2O_4 , so that they cannot be evidenced in the XRD pattern.

In case of sample P6 (with 1,3 PG) (figure 10) the lines characteristic to the spinel phase Co_3O_4 are weakly evidenced only in the XRD pattern of the sample annealed at 973 K. The strong reducing atmosphere formed during the thermal decomposition of the precursor with 1,3 PG maintains the oxidation state of CoO at low temperatures (573 K, 673 K).¹¹ This presumption explains the crystallization of Co_3O_4 at higher temperature.

Pattern (4) (figure 10) of the sample annealed at 1273 K is similar with the one presented in figure 9 (pattern (4)).

4. Conclusions

The presented study, regarding the obtaining of $\text{Co}_x\text{Fe}_{3-x}\text{O}_4$ system, has shown that the synthesis method used by us allows the preparation of cobalt ferrite CoFe_2O_4 as nanocrystallites in certain working conditions. For $x = 1$, we have obtained CoFe_2O_4 as sole nanocrystal-

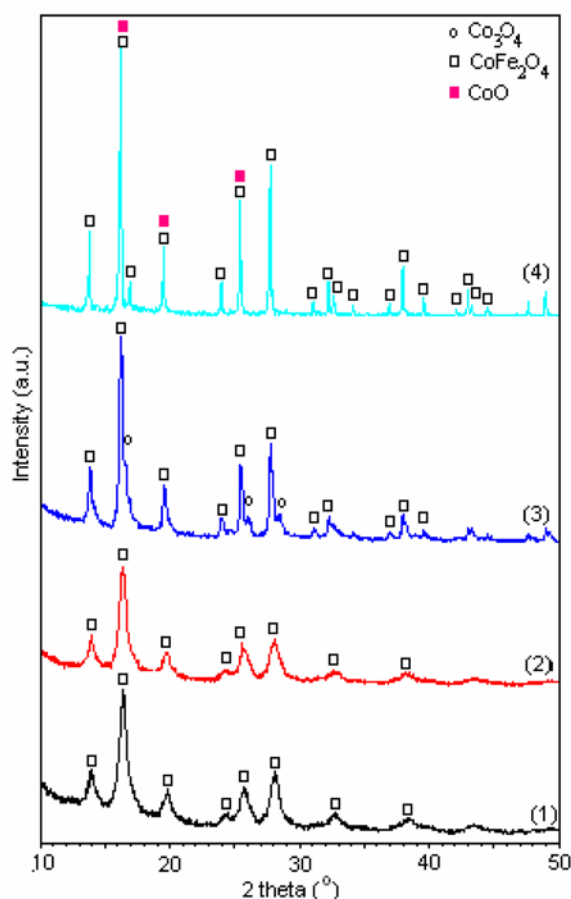


Figure 10. XRD patterns for the samples P6 annealed at different temperatures: 573 K (1); 673 K (2); 973 K (3); 1273 K (4)

line phase starting from 573 K, in case of the precursors synthesized with 1,3 propanediol. In case of the precursor synthesized with 1,2 propanediol cobalt ferrite forms quantitatively at 1273 K, due to Co_3O_4 formed at low temperatures during the decomposition of the precursor.

Independent on the precursors nature, for $x \neq 1$ ($\text{Co}_x\text{Fe}_{3-x}\text{O}_4$) we have obtained besides cobalt ferrite (CoFe_2O_4) the secondary phases: Fe_2O_3 (for $x < 1$) and Co_3O_4 (for $x > 1$).

Povzetek

Študirali smo sintezo faz oksidnega sistema $\text{Co}_x\text{Fe}_{3-x}\text{O}_4$ ($x = 0,5; 1,0; 1,5$) v obliki nanodelcev iz kovinskih nitratov ($\text{Co}(\text{NO}_3)_2 \cdot 6\text{H}_2\text{O}$, $\text{Fe}(\text{NO}_3)_3 \cdot 9\text{H}_2\text{O}$) in diolov 1,2 propanediol ($\text{OHCH}_2\text{CH}(\text{OH})\text{CH}_3$) in 1,3 propanediol ($\text{OH}(\text{CH}_2)_3\text{OH}$). Med segrevanjem raztopin nitratov in diolov poteče redoks med NO_3^- anionom in diolom z oksidacijo $-\text{CH}_2-\text{OH}$ v karboksilat $-\text{COO}^-$. Nastali karboksilat tvori z $\text{Co}(\text{II})$ in $\text{Fe}(\text{III})$ kationi koordinacijske spojine, ki so prekurzorji za $\text{Co}_x\text{Fe}_{3-x}\text{O}_4$ oksidni sistem. DTA krivulje raztopin $\text{Co}(\text{NO}_3)_2 \cdot 6\text{H}_2\text{O}$, $\text{Fe}(\text{NO}_3)_3 \cdot 9\text{H}_2\text{O}$ – diol imajo dva endotermna efekta: prvi pri ~ 343 K ustreza reakciji $\text{Fe}(\text{NO}_3)_3$ – diol in drugi pri ~ 388 K ustreza reakciji $\text{Co}(\text{NO}_3)_2$ – diol. Pri redoks reakciji nastane homogena zmes $\text{Fe}(\text{III})$ in $\text{Co}(\text{II})$ karboksilatov, ki smo jo karakterizirali s termično analizo in FT-IR. Termični razpad karboksilatov pri ~ 573 K, ki mu sledi segrevanje na 673 K, 973 K and 1273 K daje $\text{Co}_x\text{Fe}_{3-x}\text{O}_4$ kot edino ali prevladujočo nanokristalinično fazo, odvisno od x vrednosti, kot smo določili z rentgenskimi praškovnimi posnetki.

5. Acknowledgements

This work was supported by the National Project no. 71-026 NANOPART, Romanian Ministry of Education and Research.

6. References

1. K. J. Kim, H. K. Kim, Y. R. Park, G. Y. Ahn, C. S. Kim, J. Y. Park, *Hyperfine Interact.* **2006**, *69*, 1363–1369.
2. E. Mendelovici, R. Villalba, A. Sagarzazu, *Termochimica Acta* **1998**, *318*, 51–56
3. A. F. Junior, E. C. O. Lima, M. A. Novak, P. R. Wells, *J. Magn. Magn. Mater.* **2007**, *308*, 198–202
4. C. Liu, A. J. Rondione, Z. J. Zhang, *Pure Appl. Chem.* **2000**, *72*, 37–45
5. A. Franco, V. Zapf, *J. Magn. Magn. Matter.* **2008**, *320*, 709–713
6. X. Li, C. Kuntal, *J. Alloys Comp.* **2003**, *349*, 264–268
7. L. J. Cote, A. S. Teja, A. P. Wilkinson, Z. J. Zhang, *Fluid Phase Equil.* **2003**, *210*, 307–317
8. E. Chirtop, I. Mirtov, R. M. Ion, M. Iliescu, *J. Optoelectron Adv. Mater.* **2000**, *2*, 379–384
9. L. Horng, G. Chern, M. C. Chen, P. C. Kang, D. S. Lee, *J. Magn. Magn. Mater.* **2004**, *270*, 389–396
10. M. Stefanescu, T. Dippong, M. Stoia, O. Stefanescu, *J. Therm. Anal. Calorim.* **2008**, *94* in press
11. M. Stefanescu, O. Stefanescu, M. Stoia, C. Lazau, *J. Therm. Anal. Calorim.* **2007**, *88*, 27–32
12. R. Prasad, Sulaxna, A. Kumar, *J. Therm. Anal. Calorim.* **2005**, *81*, 441–450
13. M. Niculescu, N. Vaszilcsin, M. Bîrzescu, P. Budrugaec, E. Segal, *J. Therm. Anal. Calorim.* **2001**, *65*, 881–889
14. Y-L. Lee, K-W. Jun, J-Y. Park, H. S. Potdar, R. C. Chikate, *J. Industrial Eng. Chem.* **2008** *14*, 38–44
15. T-L. Lai, Y-L. Lai, C-C. Lee, Y-Y. Shu, C-B. Wang, *Catal. Today*, **2008**, *131*, 105–110
16. T. D. Glotch, R.V. Morris, P.R. Christensen, T. G. Sharp, *J. Geophys. Res.* **2004**, *109*, DOI:10.1029/2003JE002224
17. H-K. Lin, H-C. Chiu, H-C. Tsai, S-H. Chien, C-B. Wang C-B, *Catal. Let.* **2003**, *88*, 169, 3–4